

# Comparison and coupling of continuous and hybridizable discontinuous Galerkin methods: Application to multi-physics problems

Mahendra Paipuri<sup>1,2</sup>

Advisors: Prof. Carlos Tiago<sup>1</sup> and Prof. Sonia Fernández<sup>2</sup>

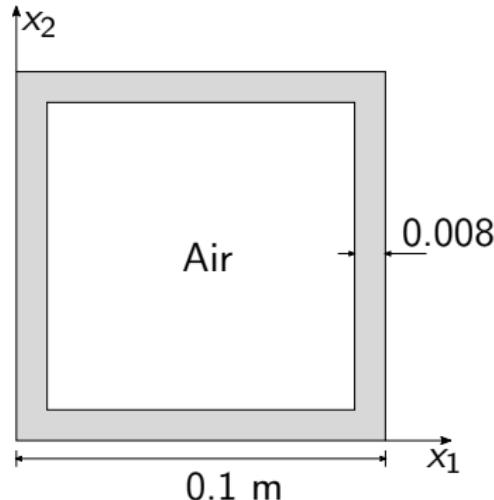
<sup>1</sup>Civil Engineering Research and Innovation for Sustainability (CERIS)  
Instituto Superior Técnico (IST)  
Universidade Lisboa



<sup>2</sup>Laboratori de Càlcul Numèric (LaCàN)  
Universitat Politècnica de Catalunya (UPC)  
Barcelona

# GFRP tubular section

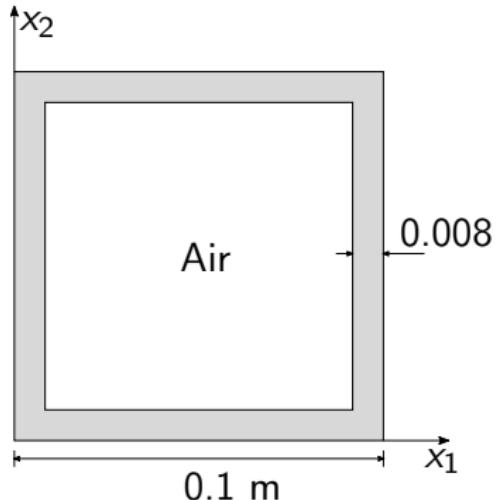
- GFRP: Glass Fiber Reinforced Polymer.
- Light, Durability, High Strength, etc.
- Fire behaviour ??



Taken from Correia et al., 2010

# GFRP tubular section

- GFRP: Glass Fiber Reinforced Polymer.
- Light, Durability, High Strength, etc.
- Fire behaviour ??



Taken from Correia et al., 2010

**Aim:** Develop an *efficient* and *robust* numerical method to solve conjugate heat transfer problems.

Incompressible Navier–Stokes equations  
+  
Convection-diffusion equation

$$\frac{\partial \mathbf{u}}{\partial t} + \operatorname{div}(\mathbf{u} \otimes \mathbf{u}) - \operatorname{div}(-p\mathbf{I} + \nu \operatorname{grad} \mathbf{u}) = \bar{\mathbf{s}},$$

$$\operatorname{div} \mathbf{u} = 0,$$

$$\frac{\partial \theta}{\partial t} + \operatorname{div}(\alpha \operatorname{grad} \theta + \mathbf{u} \theta) = \bar{g},$$

+B.C. and T.C.

Heat conduction equation for  
GFRP

$$\frac{\partial \theta}{\partial t} + \operatorname{div}(\alpha \operatorname{grad} \theta) = \bar{g},$$

+ Convection and radiation B.C.

Heat conduction equation for  
GFRP

$$\frac{\partial \theta}{\partial t} + \operatorname{div}(\alpha \operatorname{grad} \theta) = \bar{g},$$

+ Convection and radiation B.C.

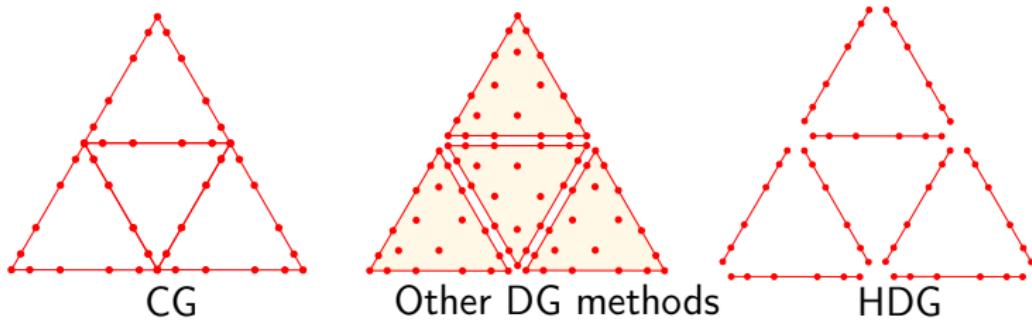
Radiosity equation

$$R = \sigma \epsilon \theta^4 + (1-\epsilon) \int_{S_R} R \frac{\cos \gamma_x \cos \gamma_\xi}{\pi r^2} dS_R.$$

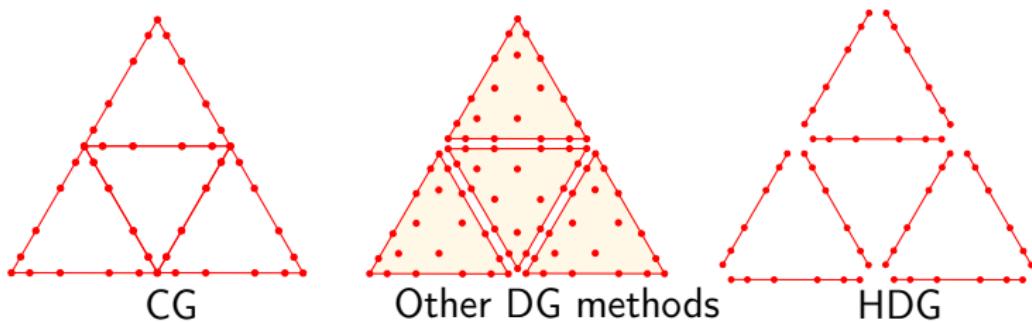
- Incompressible Navier–Stokes and convection-diffusion equation for fluid domain and heat conduction equation for solid part.
- **Radiosity** in the internal cavity must be considered.

- Incompressible Navier–Stokes and convection-diffusion equation for fluid domain and heat conduction equation for solid part.
- Radiosity in the internal cavity must be considered.
- Use *Hybridizable Discontinuous Galerkin (HDG)* to discretize the fluid part and *Continuous Galerkin (CG)* to discretize solid domain and radiosity.

- Incompressible Navier–Stokes and convection-diffusion equation for fluid domain and heat conduction equation for solid part.
- **Radiosity** in the internal cavity must be considered.
- Use *Hybridizable Discontinuous Galerkin (HDG)* to discretize the fluid part and *Continuous Galerkin (CG)* to discretize solid domain and radiosity.



- Incompressible Navier–Stokes and convection-diffusion equation for fluid domain and heat conduction equation for solid part.
- Radiosity in the internal cavity must be considered.
- Use *Hybridizable Discontinuous Galerkin (HDG)* to discretize the fluid part and *Continuous Galerkin (CG)* to discretize solid domain and radiosity.



- Computational efficiency of **HDG** vs. **CG** for incompressible fluid flow problems ??

# Plan

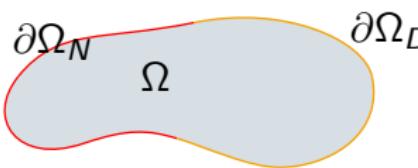
- 1 Comparison of HDG and CG for incompressible Navier–Stokes
  - HDG for incompressible Navier–Stokes
  - Comparison of CPU times
  - Comparison of stability in presence of sharp fronts
- 2 Coupling of CG and HDG for heat equation
  - Coupled CG-HDG formulation for heat equation
  - Application of coupled formulation for conjugate heat transfer problem
- 3 Application to GFRP tubular cross-section
  - Problem statement
  - Radiosity
  - Numerical results
- 4 Summary

# Plan

- 1 Comparison of HDG and CG for incompressible Navier–Stokes
  - HDG for incompressible Navier–Stokes
  - Comparison of CPU times
  - Comparison of stability in presence of sharp fronts
- 2 Coupling of CG and HDG for heat equation
  - Coupled CG-HDG formulation for heat equation
  - Application of coupled formulation for conjugate heat transfer problem
- 3 Application to GFRP tubular cross-section
  - Problem statement
  - Radiosity
  - Numerical results
- 4 Summary

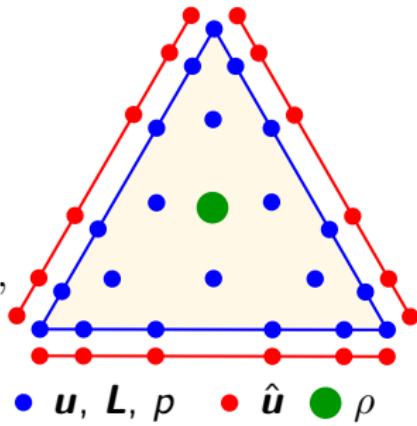
# Steady incompressible Navier–Stokes equations

$$\begin{aligned} \operatorname{div}(\mathbf{u} \otimes \mathbf{u}) - \operatorname{div}(-p\mathbf{I} + \nu \operatorname{grad} \mathbf{u}) &= \bar{\mathbf{s}} && \text{in } \Omega, \\ \operatorname{div} \mathbf{u} &= 0 && \text{in } \Omega, \\ \mathbf{u} &= \bar{\mathbf{u}} && \text{on } \partial\Omega_D, \\ (-p\mathbf{I} + \nu \operatorname{grad} \mathbf{u}) \mathbf{n} &= \bar{\mathbf{t}} && \text{on } \partial\Omega_N, \end{aligned}$$



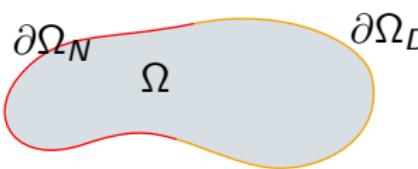
*Local problem*

$$\begin{aligned} \mathbf{L} - \operatorname{grad} \mathbf{u} &= \mathbf{0} && \text{in } \Omega^e, \\ \operatorname{div}(\mathbf{u} \otimes \mathbf{u}) - \operatorname{div}(-p\mathbf{I} + \nu \mathbf{L}) &= \bar{\mathbf{s}} && \text{in } \Omega^e, \\ \operatorname{div} \mathbf{u} &= 0 && \text{in } \Omega^e, \\ \mathbf{u} &= \hat{\mathbf{u}} && \text{on } \partial\Omega^e, \\ \frac{1}{|\partial\Omega^e|} \langle p, 1 \rangle_{\partial\Omega^e} &= \rho_e && \end{aligned}$$



# Steady incompressible Navier–Stokes equations

$$\begin{aligned} \operatorname{div}(\mathbf{u} \otimes \mathbf{u}) - \operatorname{div}(-p\mathbf{I} + \nu \operatorname{grad} \mathbf{u}) &= \bar{\mathbf{s}} && \text{in } \Omega, \\ \operatorname{div} \mathbf{u} &= 0 && \text{in } \Omega, \\ \mathbf{u} &= \bar{\mathbf{u}} && \text{on } \partial\Omega_D, \\ (-p\mathbf{I} + \nu \operatorname{grad} \mathbf{u}) \mathbf{n} &= \bar{\mathbf{t}} && \text{on } \partial\Omega_N, \end{aligned}$$



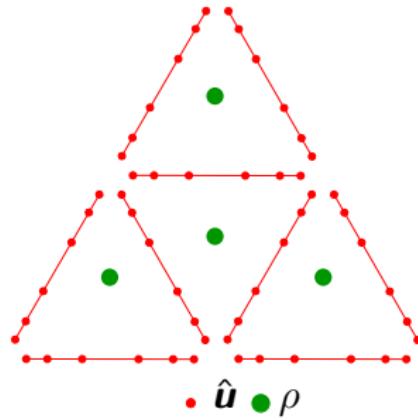
*Global problem*

$$[(-p\mathbf{I} + \nu \mathbf{L}) \mathbf{n}] = \mathbf{0} \quad \text{on } \Gamma \setminus \partial\Omega,$$

$$\langle \hat{\mathbf{u}} \cdot \mathbf{n} \rangle_{\partial\Omega^e} = 0,$$

$$\hat{\mathbf{u}} = \bar{\mathbf{u}} \quad \text{on } \partial\Omega_D.$$

$$\text{where } \Gamma = \bigcup_{e=1}^{n_{el}} \partial\Omega^e$$



# Discretized system

- In the linearised system, *Local Solver* can be expressed as,

$$\begin{bmatrix} \delta\mathbf{u} \\ \delta\mathbf{L} \\ \delta\mathbf{p} \end{bmatrix} = - \begin{bmatrix} \mathbf{A}_{uu}(\mathbf{u}) & \mathbf{A}_{uL} & \mathbf{A}_{up} \\ \mathbf{A}_{Lu} & \mathbf{A}_{LL} & \\ \mathbf{A}_{pu} & & \end{bmatrix}^{-1} \left( \begin{bmatrix} \mathbf{r}_u \\ \mathbf{r}_L \\ \mathbf{r}_p \end{bmatrix} + \begin{bmatrix} \mathbf{A}_{u\hat{u}}(\hat{\mathbf{u}}) \\ \mathbf{A}_{L\hat{u}} \\ \mathbf{A}_{p\hat{u}} \end{bmatrix} \begin{bmatrix} \delta\hat{\mathbf{u}}_{F1} \\ \delta\hat{\mathbf{u}}_{F2} \\ \delta\hat{\mathbf{u}}_{F3} \end{bmatrix} \right)$$

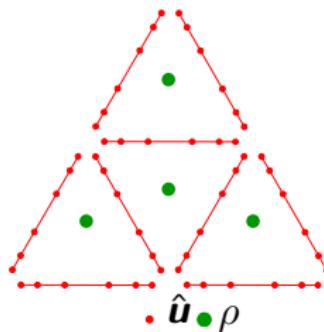
# Discretized system

- In the linearised system, *Local Solver* can be expressed as,

$$\begin{bmatrix} \delta\mathbf{u} \\ \delta\mathbf{L} \\ \delta\mathbf{p} \end{bmatrix} = - \begin{bmatrix} \mathbf{A}_{uu}(\mathbf{u}) & \mathbf{A}_{uL} & \mathbf{A}_{up} \\ \mathbf{A}_{Lu} & \mathbf{A}_{LL} & \\ \mathbf{A}_{pu} & & \end{bmatrix}^{-1} \left( \begin{bmatrix} \mathbf{r}_u \\ \mathbf{r}_L \\ \mathbf{r}_p \end{bmatrix} + \begin{bmatrix} \mathbf{A}_{u\hat{\mathbf{u}}}(\hat{\mathbf{u}}) \\ \mathbf{A}_{L\hat{\mathbf{u}}} \\ \mathbf{A}_{p\hat{\mathbf{u}}} \end{bmatrix} \begin{bmatrix} \delta\hat{\mathbf{u}}_{F1} \\ \delta\hat{\mathbf{u}}_{F2} \\ \delta\hat{\mathbf{u}}_{F3} \end{bmatrix} \right)$$

- By replacing  $\delta\mathbf{u}, \delta\mathbf{L}, \delta\mathbf{p}$  using local solver, the discretized *Global Solver* can be expressed as,

$$\begin{bmatrix} \mathbf{A}_{\hat{\mathbf{u}}\hat{\mathbf{u}}}(\hat{\mathbf{u}}) & \mathbf{A}_{\rho\hat{\mathbf{u}}}^T \\ \mathbf{A}_{\rho\hat{\mathbf{u}}} & \end{bmatrix} \begin{bmatrix} \delta\hat{\mathbf{u}} \\ \delta\rho \end{bmatrix} = \begin{bmatrix} \mathbf{s} \\ \mathbf{0} \end{bmatrix}$$



- Local variables can be computed using local solver and  $\delta\hat{\mathbf{u}}, \delta\rho$ .

## Post-processed solution

- Velocity, gradient of velocity and pressure converges with optimal rate of  $k + 1$ , if  $k$  is the degree of approximation.

# Post-processed solution

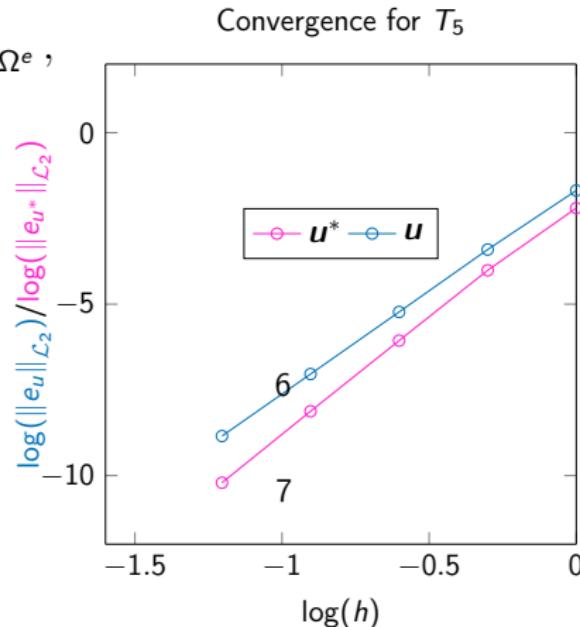
- Velocity, gradient of velocity and pressure converges with optimal rate of  $k + 1$ , if  $k$  is the degree of approximation.
- Mean of velocity in the each element converges with a rate of  $k + 2$ .

# Post-processed solution

- Velocity, gradient of velocity and pressure converges with optimal rate of  $k+1$ , if  $k$  is the degree of approximation.
- Mean of velocity in the each element converges with a rate of  $k+2$ .

$$\begin{aligned} (\operatorname{grad} \delta \boldsymbol{u}^*, \operatorname{grad} \boldsymbol{u}^*)_{\Omega^e} &= (\operatorname{grad} \delta \boldsymbol{u}^*, \boldsymbol{L})_{\Omega^e}, \\ (\boldsymbol{u}^*, 1)_{\Omega^e} &= (\boldsymbol{u}, 1)_{\Omega^e}. \end{aligned}$$

- The new  $\boldsymbol{u}^*$  converges with an order of  $k+2$ . Computations are performed element-by-element.

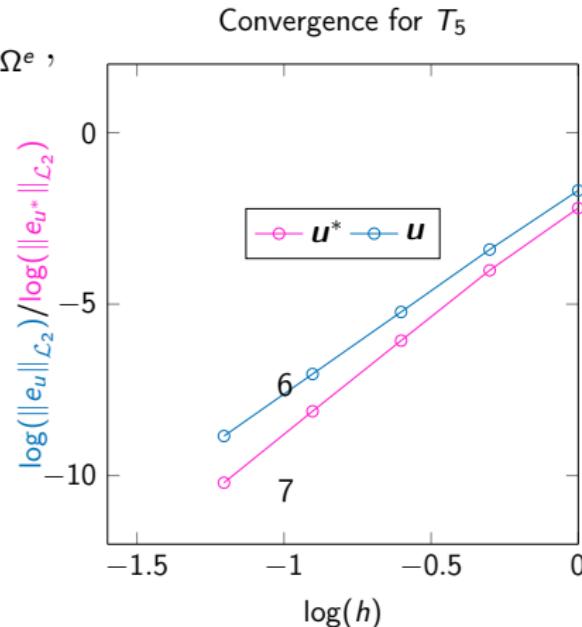


# Post-processed solution

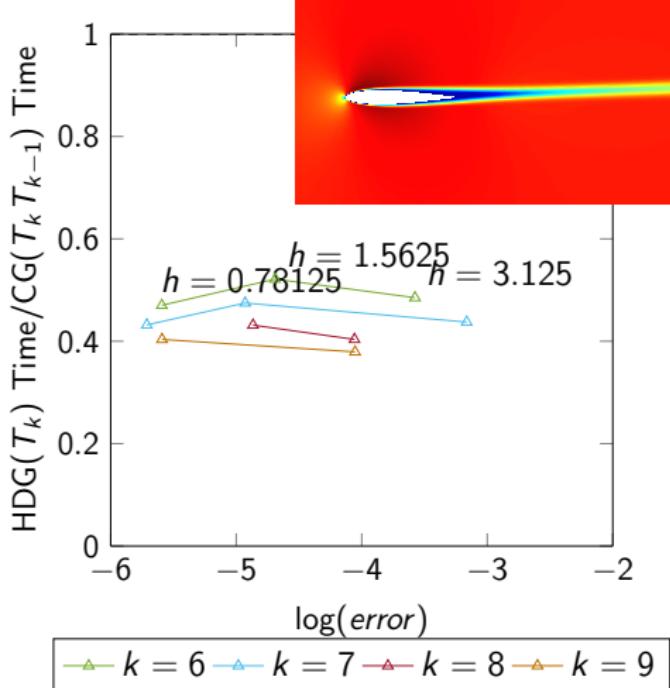
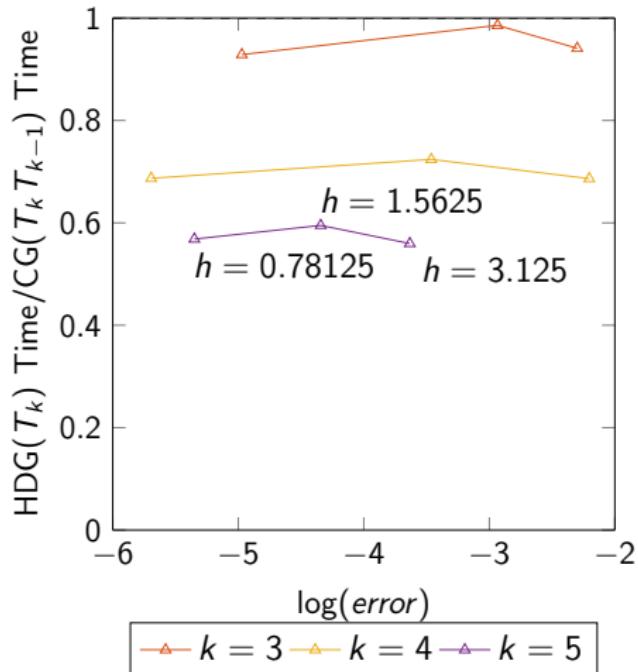
- Velocity, gradient of velocity and pressure converges with optimal rate of  $k+1$ , if  $k$  is the degree of approximation.
- Mean of velocity in the each element converges with a rate of  $k+2$ .

$$\begin{aligned} (\operatorname{grad} \delta \boldsymbol{u}^*, \operatorname{grad} \boldsymbol{u}^*)_{\Omega^e} &= (\operatorname{grad} \delta \boldsymbol{u}^*, \boldsymbol{L})_{\Omega^e}, \\ (\boldsymbol{u}^*, 1)_{\Omega^e} &= (\boldsymbol{u}, 1)_{\Omega^e}. \end{aligned}$$

- The new  $\boldsymbol{u}^*$  converges with an order of  $k+2$ . Computations are performed **element-by-element**.
- Super-convergence has only been proven in **diffusive** regime.



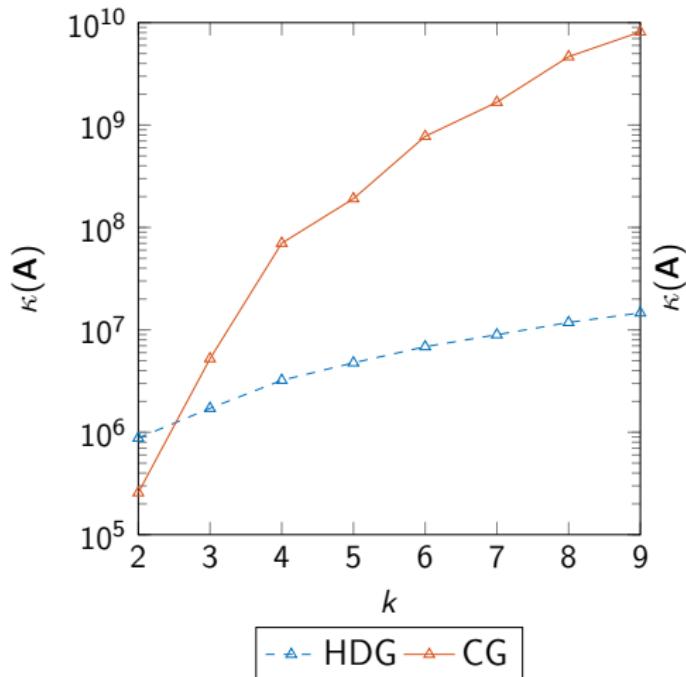
# Ratio of CPU times vs. error for NACA0012 airfoil



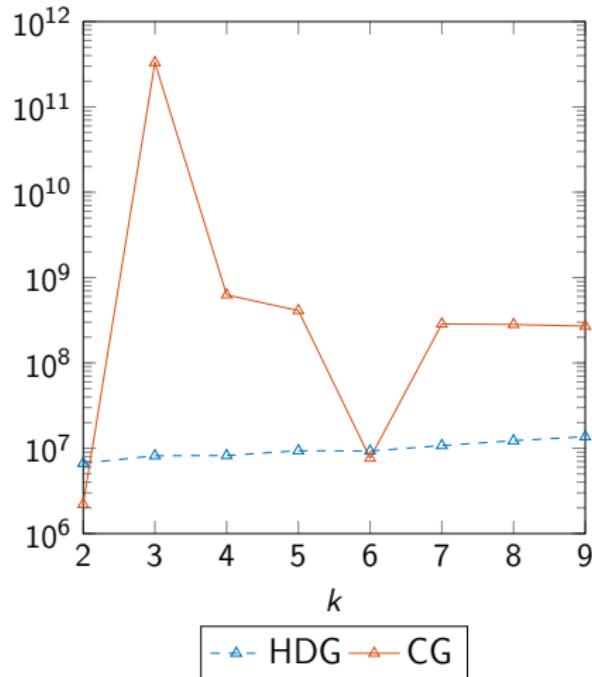
Similar study is done for NACA0012 airfoil example using Navier–Stokes equations. Error in lift coefficient is used.

# Condition numbers

Kovaszany flow,  $n_{el} = 8\,192$

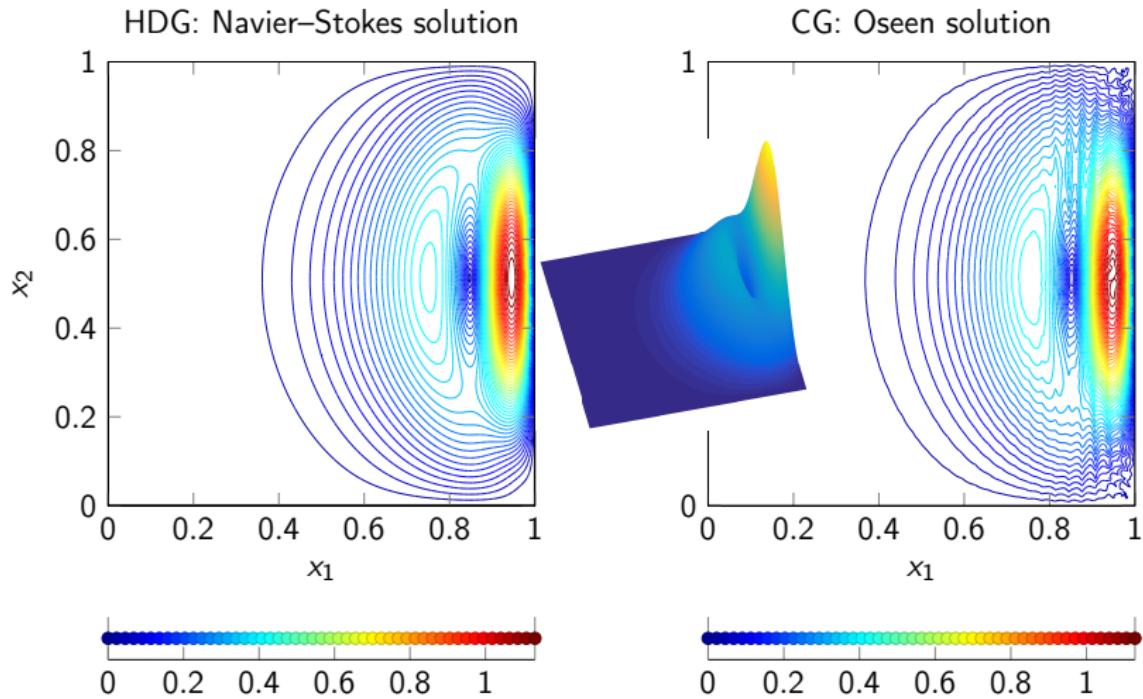


NACA0012,  $n_{el} = 8\,192$



Most of the cases, HDG produces *better conditioned* matrix than CG in both Stokes and Navier–Stokes.

# Sharp front test: Isolines of velocity field at $Re = 2000$



The non-linear solver in CG *fails* to converge. Oseen solution is computed for CG to show the numerical instabilities.

# Conclusions

- HDG has **similar or superior** computational efficiency than CG for incompressible flow problems.
- In presence of sharp fronts, it is shown that HDG exhibits superior stability properties than CG.
- Summing up, HDG has **super-convergence in low  $Re$  regimes and better stability at higher  $Re$ .**

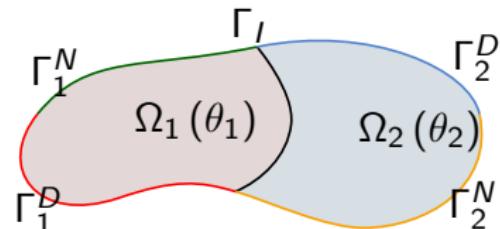
# Plan

- 1 Comparison of HDG and CG for incompressible Navier–Stokes
  - HDG for incompressible Navier–Stokes
  - Comparison of CPU times
  - Comparison of stability in presence of sharp fronts
- 2 Coupling of CG and HDG for heat equation
  - Coupled CG-HDG formulation for heat equation
  - Application of coupled formulation for conjugate heat transfer problem
- 3 Application to GFRP tubular cross-section
  - Problem statement
  - Radiosity
  - Numerical results
- 4 Summary

# Strong formulation for coupled CG-HDG model

Coupling formulation is presented in the framework of *second-order elliptic operators*.

$$\begin{aligned}
 \mathbf{q}_1 + (\alpha_1 \operatorname{grad} \theta_1) &= \mathbf{0} && \text{in } \Omega_1, \\
 \operatorname{div} \mathbf{q}_1 &= \bar{g}_1 && \text{in } \Omega_1, \\
 -\operatorname{div} (\alpha_2 \operatorname{grad} \theta_2) &= \bar{g}_2 && \text{in } \Omega_2, \\
 \theta_1 &= \bar{\theta}_1 && \text{on } \Gamma_1^D, \\
 \theta_2 &= \bar{\theta}_2 && \text{on } \Gamma_2^D, \\
 \theta_1 - \theta_2 &= 0 && \text{on } \Gamma_I, \\
 \mathbf{q}_1 \cdot \mathbf{n}_1 - (\alpha_2 \operatorname{grad} \theta_2) \cdot \mathbf{n}_2 &= 0 && \text{on } \Gamma_I,
 \end{aligned}$$



**Notation:**

$$\Gamma_1 = \bigcup_{e=1}^{m_{el}} \partial\Omega_1^e, \quad \Gamma_2 = \bigcup_{e=1}^{p_{el}} \partial\Omega_2^e.$$

# Proposed coupling

## Transmission conditions

$$\begin{aligned}\theta_1 - \theta_2 &= 0 \text{ on } \Gamma_I, \\ \mathbf{q}_1 \cdot \mathbf{n}_1 - (\alpha_2 \operatorname{grad} \theta_2) \cdot \mathbf{n}_2 &= 0 \text{ on } \Gamma_I,\end{aligned}$$

# Proposed coupling

## Transmission conditions

$$\hat{\theta}_1 - \theta_2 = 0 \text{ on } \Gamma_I,$$

$$\hat{\mathbf{q}}_1 \cdot \mathbf{n}_1 - (\alpha_2 \operatorname{grad} \theta_2) \cdot \mathbf{n}_2 = 0 \text{ on } \Gamma_I.$$

# Proposed coupling

## Transmission conditions

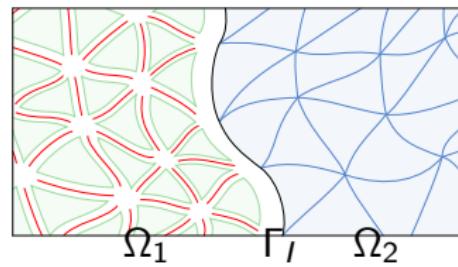
$$\hat{\theta}_1 - \theta_2 = 0 \text{ on } \Gamma_I,$$

$$\hat{\mathbf{q}}_1 \cdot \mathbf{n}_1 - (\alpha_2 \operatorname{grad} \theta_2) \cdot \mathbf{n}_2 = 0 \text{ on } \Gamma_I.$$

## Definition of trace and numerical flux

$$\theta_1 = \begin{cases} \hat{\theta}_1 & \text{on } \partial\Omega_1^e \setminus \Gamma_I, \\ \theta_2 & \text{on } \partial\Omega_1^e \cap \Gamma_I, \end{cases}$$

$$\hat{\mathbf{q}}_1 \cdot \mathbf{n}_1 = \begin{cases} \mathbf{q}_1 \cdot \mathbf{n}_1 + \tau(\theta_1 - \hat{\theta}_1) & \text{on } \partial\Omega_1^e \setminus \Gamma_I, \\ \mathbf{q}_1 \cdot \mathbf{n}_1 + \tau(\theta_1 - \theta_2) & \text{on } \partial\Omega_1^e \cap \Gamma_I. \end{cases}$$



## Weak form of HDG local problem

$$\begin{aligned}
 & (\delta\theta_1, \operatorname{div} \mathbf{q}_1)_{\Omega_1^e} + \left\langle \delta\theta_1, \tau(\theta_1 - \hat{\theta}_1) \right\rangle_{\partial\Omega_1^e \setminus \Gamma_I} \\
 & \quad + \langle \delta\theta_1, \tau(\theta_1 - \theta_2) \rangle_{\partial\Omega_1^e \cap \Gamma_I} - (\delta\theta_1, \bar{g}_1)_{\Omega_1^e} = 0, \\
 & (\delta\mathbf{q}_1, \alpha_1^{-1} \mathbf{q}_1)_{\Omega_1^e} - (\operatorname{div} \delta\mathbf{q}_1, \theta_1)_{\Omega_1^e} + \left\langle \delta\mathbf{q}_1 \cdot \mathbf{n}, \hat{\theta}_1 \right\rangle_{\partial\Omega_1^e \setminus \Gamma_I} \\
 & \quad + \langle \delta\mathbf{q}_1 \cdot \mathbf{n}_1, \theta_2 \rangle_{\partial\Omega_1^e \cap \Gamma_I} = 0,
 \end{aligned}$$

for  $e = 1, \dots, m_{el}$

## Weak form of HDG global problem

$$\sum_{e=1}^{m_{el}} \left\langle \delta\hat{\theta}_1, \left( \mathbf{q}_1 \cdot \mathbf{n} + \tau(\theta_1 - \hat{\theta}_1) \right) \right\rangle_{\partial\Omega_1^e \setminus \Gamma_I} = 0,$$

## Weak form of CG

$$\begin{aligned}
 & (\operatorname{grad} \delta\theta_2, \alpha_2 \operatorname{grad} \theta_2)_{\Omega_2} - \langle \delta\theta_2, \mathbf{q}_1 \cdot \mathbf{n}_1 \rangle_{\Gamma_I} \\
 & \quad + \langle \delta\theta_2, \tau(\theta_1 - \theta_2) \rangle_{\Gamma_I} - (\delta\theta_2, \bar{g}_2)_{\Omega_2} = 0.
 \end{aligned}$$

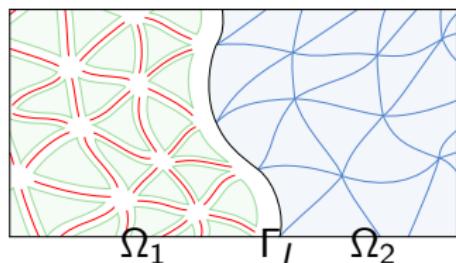
# Proposed coupling

## Transmission conditions

$$\begin{aligned}\hat{\theta}_1 - \theta_2 &= 0 \text{ on } \Gamma_I, \\ \hat{\mathbf{q}}_1 \cdot \mathbf{n}_1 - (\alpha_2 \operatorname{grad} \theta_2) \cdot \mathbf{n}_2 &= 0 \text{ on } \Gamma_I.\end{aligned}$$

## Definition of trace and numerical flux

$$\begin{aligned}\theta_1 &= \begin{cases} \hat{\theta}_1 & \text{on } \partial\Omega_1^e \setminus \Gamma_I, \\ \theta_2 & \text{on } \partial\Omega_1^e \cap \Gamma_I, \end{cases} \\ \hat{\mathbf{q}}_1 \cdot \mathbf{n}_1 &= \begin{cases} \mathbf{q}_1 \cdot \mathbf{n}_1 + \tau(\theta_1 - \hat{\theta}_1) & \text{on } \partial\Omega_1^e \setminus \Gamma_I, \\ \mathbf{q}_1 \cdot \mathbf{n}_1 + \tau(\theta_1 - \theta_2) & \text{on } \partial\Omega_1^e \cap \Gamma_I. \end{cases}\end{aligned}$$



## Discretized system

$$\left[ \begin{array}{cc|cc} \mathbf{A}_{\hat{\theta}\hat{\theta}} & \mathbf{0} & \mathbf{A}_{\hat{\theta}\theta} & \mathbf{A}_{\hat{\theta}q} \\ \mathbf{0} & \mathbf{K}_{\theta\theta} & \mathbf{B}_{\theta\theta}^T & \mathbf{B}_{\theta q} \\ \hline \mathbf{A}_{\theta\hat{\theta}} & \mathbf{B}_{\theta\theta} & \mathbf{A}_{\theta\theta} & \mathbf{A}_{\theta q} \\ \mathbf{A}_{q\hat{\theta}} & \mathbf{B}_{q\theta} & \mathbf{A}_{q\theta} & \mathbf{A}_{qq} \end{array} \right] \left\{ \begin{array}{c} \hat{\theta}_1 \\ \theta_2 \\ \theta_1 \\ \mathbf{q}_1 \end{array} \right\} = \left\{ \begin{array}{c} \mathbf{0} \\ \bar{\mathbf{g}}_2 \\ \bar{\mathbf{g}}_1 \\ \mathbf{0} \end{array} \right\}.$$

# Alternative coupling

## Transmission conditions

$$\begin{aligned}\hat{\theta}_1 - \theta_2 &= 0 \text{ on } \Gamma_I, \\ \hat{\mathbf{q}}_1 \cdot \mathbf{n}_1 - (\alpha_2 \operatorname{grad} \theta_2) \cdot \mathbf{n}_2 &= 0 \text{ on } \Gamma_I.\end{aligned}$$

# Alternative coupling

## Transmission conditions

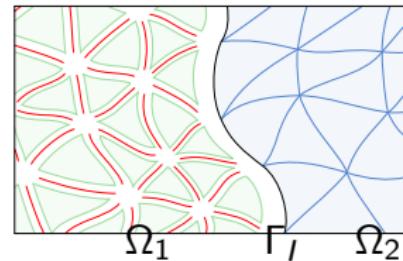
$$\hat{\theta}_1 - \theta_2 = 0 \text{ on } \Gamma_I,$$

$$\hat{\mathbf{q}}_1 \cdot \mathbf{n}_1 - (\alpha_2 \operatorname{grad} \theta_2) \cdot \mathbf{n}_2 = 0 \text{ on } \Gamma_I.$$

## Definition of trace and numerical flux

$$\theta_1 = \begin{cases} \hat{\theta}_1 & \text{on } \partial\Omega_1^e \setminus \Gamma_I, \\ \mathbb{P}_2(\theta_2) & \text{on } \partial\Omega_1^e \cap \Gamma_I, \end{cases}$$

$$\hat{\mathbf{q}}_1 \cdot \mathbf{n}_1 = \begin{cases} \mathbf{q}_1 \cdot \mathbf{n}_1 + \tau(\theta_1 - \hat{\theta}_1) & \text{on } \partial\Omega_1^e \setminus \Gamma_I, \\ \mathbf{q}_1 \cdot \mathbf{n}_1 + \tau(\theta_1 - \mathbb{P}_2(\theta_2)) & \text{on } \partial\Omega_1^e \cap \Gamma_I. \end{cases}$$



# Alternative coupling

## Transmission conditions

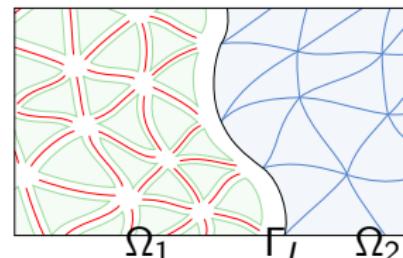
$$\hat{\theta}_1 - \theta_2 = 0 \text{ on } \Gamma_I,$$

$$\hat{\mathbf{q}}_1 \cdot \mathbf{n}_1 - (\alpha_2 \operatorname{grad} \theta_2) \cdot \mathbf{n}_2 = 0 \text{ on } \Gamma_I.$$

## Definition of trace and numerical flux

$$\theta_1 = \begin{cases} \hat{\theta}_1 & \text{on } \partial\Omega_1^e \setminus \Gamma_I, \\ \mathbb{P}_2(\theta_2) & \text{on } \partial\Omega_1^e \cap \Gamma_I, \end{cases}$$

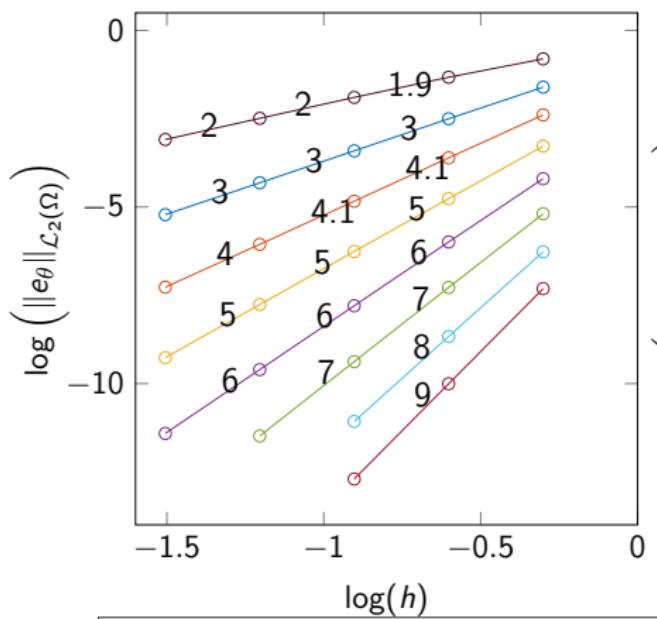
$$\hat{\mathbf{q}}_1 \cdot \mathbf{n}_1 = \begin{cases} \mathbf{q}_1 \cdot \mathbf{n}_1 + \tau(\theta_1 - \hat{\theta}_1) & \text{on } \partial\Omega_1^e \setminus \Gamma_I, \\ \mathbf{q}_1 \cdot \mathbf{n}_1 + \tau(\theta_1 - \mathbb{P}_2(\theta_2)) & \text{on } \partial\Omega_1^e \cap \Gamma_I. \end{cases}$$



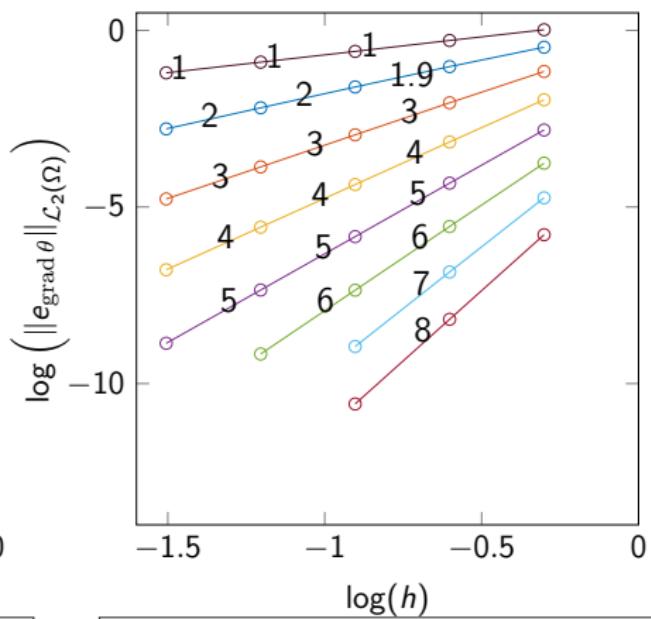
## Discretized system

$$\left[ \begin{array}{ccc|cc} \mathbf{A}_{\hat{\theta}\hat{\theta}} & 0 & 0 & \mathbf{A}_{\hat{\theta}\theta} & \mathbf{A}_{\hat{\theta}q} \\ 0 & \mathbf{P}^T \mathbf{A}_{\hat{\theta}\hat{\theta}} \mathbf{P} + \mathbf{K}_{\theta\theta}^{II} & \mathbf{K}_{\theta\theta}^{li} & \mathbf{P}^T \mathbf{A}_{\hat{\theta}\theta} & \mathbf{P}^T \mathbf{A}_{\hat{\theta}q} \\ 0 & \mathbf{K}_{\theta\theta}^{il} & \mathbf{K}_{\theta\theta}^{ii} & 0 & 0 \\ \hline \mathbf{A}_{\theta\hat{\theta}} & \mathbf{A}_{\theta\hat{\theta}} \mathbf{P} & 0 & \mathbf{A}_{\theta\theta} & \mathbf{A}_{\theta q} \\ \mathbf{A}_{q\hat{\theta}} & \mathbf{A}_{q\hat{\theta}} \mathbf{P} & 0 & \mathbf{A}_{q\theta} & \mathbf{A}_{qq} \end{array} \right] \begin{Bmatrix} \hat{\theta}_1 \\ \theta_2' \\ \theta_2^i \\ \theta_1 \\ \mathbf{q}_1 \end{Bmatrix} = \begin{Bmatrix} 0 \\ \bar{\mathbf{g}}_2^l \\ \bar{\mathbf{g}}_2^i \\ \bar{\mathbf{g}}_1 \\ 0 \end{Bmatrix},$$

# Convergence for coupled $\text{CG}(T_k)$ - $\text{HDG}(T_k)$ model

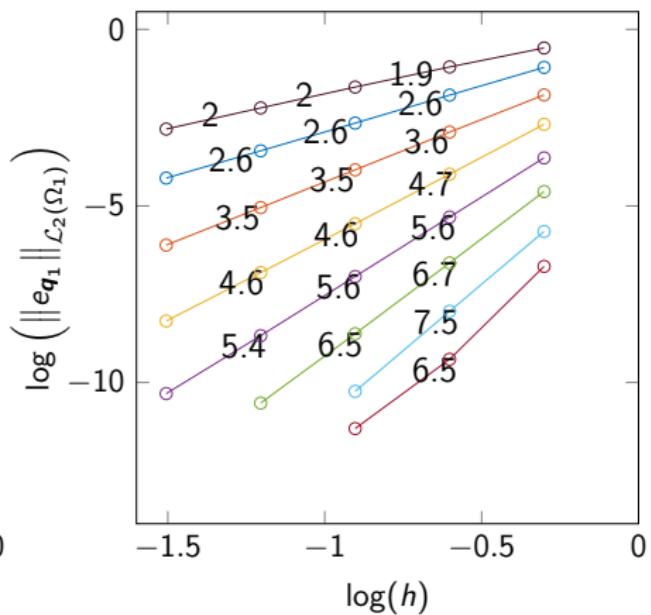
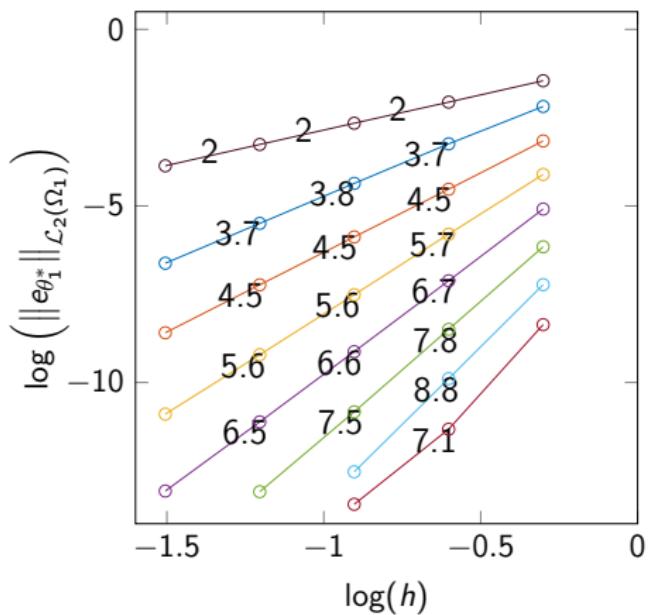


—○—  $k = 1$   
 —○—  $k = 2$   
 —○—  $k = 3$   
 —○—  $k = 4$   
—○—  $k = 5$   
 —○—  $k = 6$   
 —○—  $k = 7$   
 —○—  $k = 8$



—○—  $k = 1$   
 —○—  $k = 2$   
 —○—  $k = 3$   
 —○—  $k = 4$   
—○—  $k = 5$   
 —○—  $k = 6$   
 —○—  $k = 7$   
 —○—  $k = 8$

# Coupled $\text{CG}(T_k)$ - $\text{HDG}(T_k)$ model: Error in $\Omega_1$



Legend:

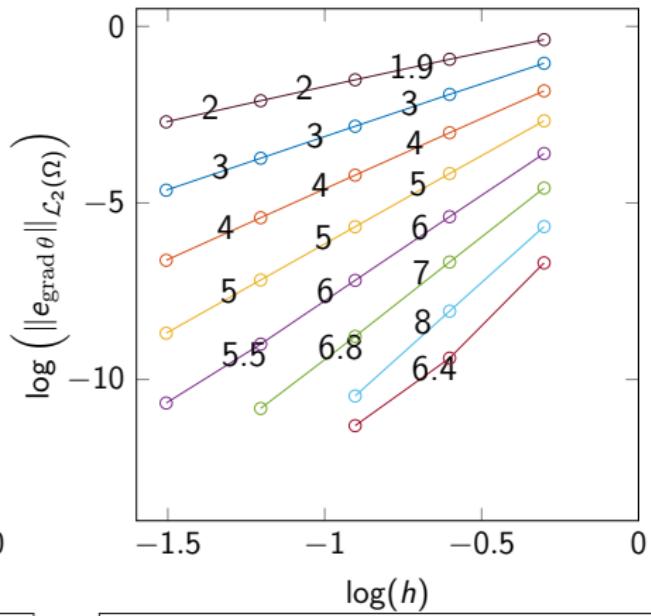
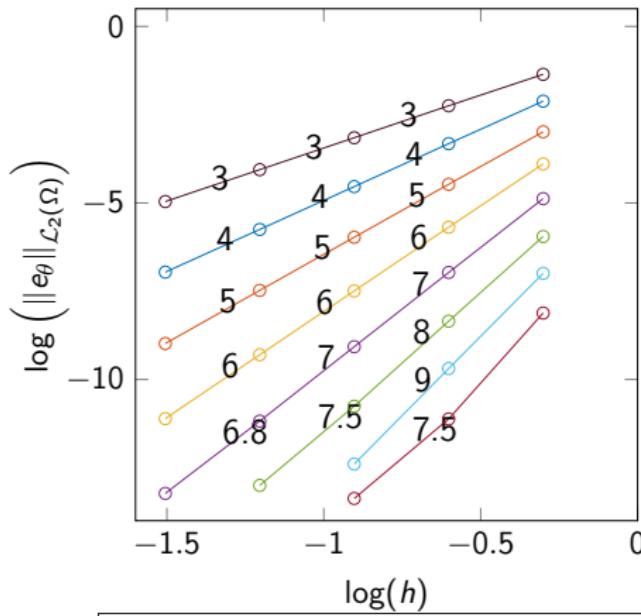
- $\circ - k = 1$     $\circ - k = 2$     $\circ - k = 3$     $\circ - k = 4$
- $\circ - k = 5$     $\circ - k = 6$     $\circ - k = 7$     $\circ - k = 8$

Legend:

- $\circ - k = 1$     $\circ - k = 2$     $\circ - k = 3$     $\circ - k = 4$
- $\circ - k = 5$     $\circ - k = 6$     $\circ - k = 7$     $\circ - k = 8$

HDG post-processed solution *lost the optimal convergence* for this approximation. Rate is  $k + 1.5$  instead of  $k + 2$ .

# Convergence for coupled $\text{CG}(T_{k+1})\text{-HDG}(T_k)$ model



—○—  $k = 1$   
 —○—  $k = 2$   
 —○—  $k = 3$   
 —○—  $k = 4$   
—○—  $k = 5$   
 —○—  $k = 6$   
 —○—  $k = 7$   
 —○—  $k = 8$

—○—  $k = 1$   
 —○—  $k = 2$   
 —○—  $k = 3$   
 —○—  $k = 4$   
—○—  $k = 5$   
 —○—  $k = 6$   
 —○—  $k = 7$   
 —○—  $k = 8$

This coupled model has optimal rate of  $k+2$  for temperature and  $k+1$  for gradient of temperature.

# Governing equations of conjugate heat transfer problem

$$\mathbf{L} - \operatorname{grad} \mathbf{u} = \mathbf{0} \quad \text{in } \Omega_1,$$

$$\operatorname{div} (\mathbf{u} \otimes \mathbf{u}) - \operatorname{div} (-p\mathbf{I} + \nu \mathbf{L})$$

$$-\mathbf{f}(\theta_1) = \bar{\mathbf{s}} \quad \text{in } \Omega_1,$$

$$\operatorname{div} \mathbf{u} = 0 \quad \text{in } \Omega_1,$$

$$\mathbf{q}_1 + \alpha_1 \operatorname{grad} \theta_1 = \mathbf{0} \quad \text{in } \Omega_1,$$

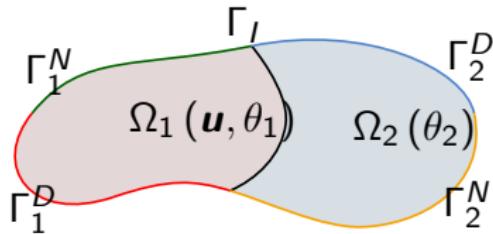
$$\operatorname{div} (\mathbf{q}_1 + \mathbf{u} \theta_1) = \bar{g}_1 \quad \text{in } \Omega_1,$$

$$-\operatorname{div} (\alpha_2 \operatorname{grad} \theta_2) = \bar{g}_2 \quad \text{in } \Omega_2,$$

$$\theta_1 - \theta_2 = 0 \quad \text{on } \Gamma_I,$$

$$\mathbf{q}_1 \cdot \mathbf{n}_1 - (\alpha_2 \operatorname{grad} \theta_2) \cdot \mathbf{n}_2 = 0 \quad \text{on } \Gamma_I.$$

+ B.C.,



# Governing equations of conjugate heat transfer problem

$$\mathbf{L} - \operatorname{grad} \mathbf{u} = \mathbf{0} \quad \text{in } \Omega_1,$$

$$\operatorname{div}(\mathbf{u} \otimes \mathbf{u}) - \operatorname{div}(-p\mathbf{I} + \nu \mathbf{L})$$

$$-\mathbf{f}(\theta_1) = \bar{\mathbf{s}} \quad \text{in } \Omega_1,$$

$$\operatorname{div} \mathbf{u} = 0 \quad \text{in } \Omega_1,$$

$$\mathbf{q}_1 + \alpha_1 \operatorname{grad} \theta_1 = \mathbf{0} \quad \text{in } \Omega_1,$$

$$\operatorname{div}(\mathbf{q}_1 + \mathbf{u} \theta_1) = \bar{g}_1 \quad \text{in } \Omega_1,$$

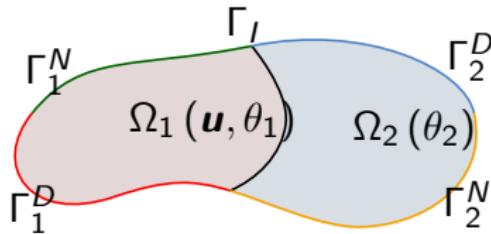
$$-\operatorname{div}(\alpha_2 \operatorname{grad} \theta_2) = \bar{g}_2 \quad \text{in } \Omega_2,$$

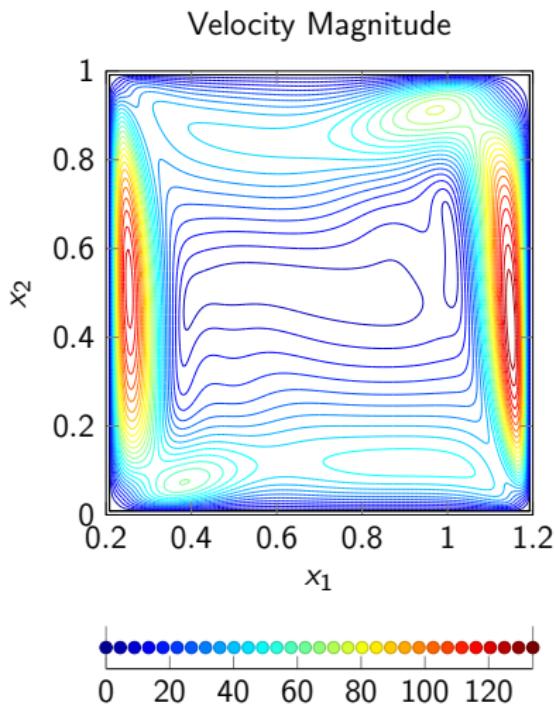
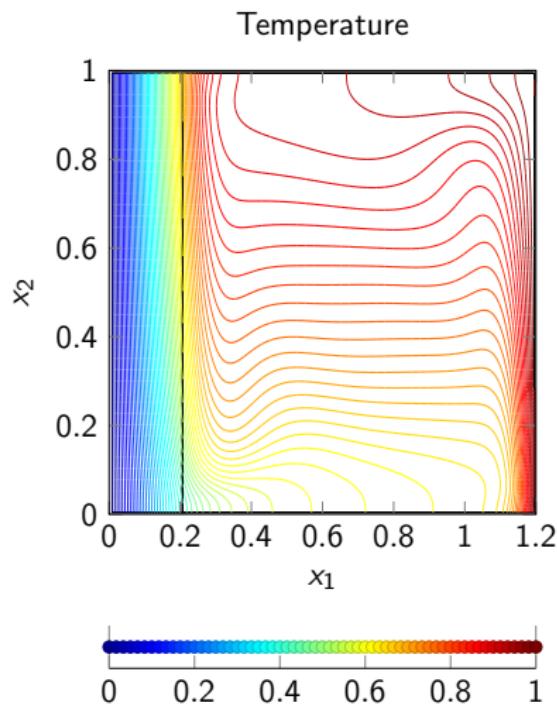
$$\theta_1 - \theta_2 = 0 \quad \text{on } \Gamma_I,$$

$$\mathbf{q}_1 \cdot \mathbf{n}_1 - (\alpha_2 \operatorname{grad} \theta_2) \cdot \mathbf{n}_2 = 0 \quad \text{on } \Gamma_I.$$

+ B.C.,

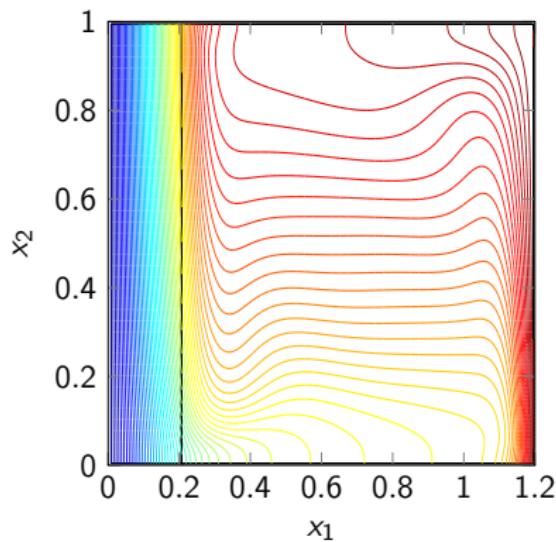
Boussinesq approximation is used to compute  $\mathbf{f}(\theta_1) = -\mathbf{g}\beta(\theta - \theta_0)$ .



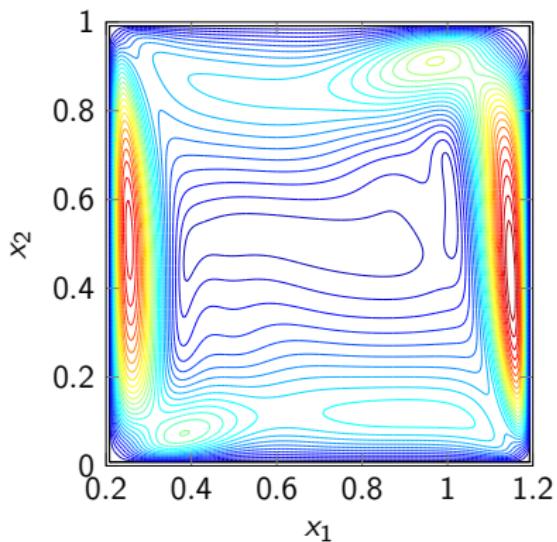
Conjugate heat transfer benchmark problem at  $Ra = 10^6$ 

Conjugate heat transfer benchmark problem at  $Ra = 10^6$ 

Temperature



Velocity Magnitude



Quantity	Misra (1997)	$CG(Q_6)$ -HDG( $Q_5$ ) or $CG(Q_6)$ -CG( $Q_6 Q_5$ )
$Nu$	2.9528	2.9605

# Conclusions

- Optimal convergence is obtained for proposed CG-HDG coupling for heat equation.
- Gain in computational efficiency is noticed using coupled CG-HDG compared to coupled CG-CG model for conjugate heat transfer problems.
- Proposed CG-HDG and HDG-HDG coupled models have computationally similar performance and accuracy for the considered examples.

# Plan

- 1 Comparison of HDG and CG for incompressible Navier–Stokes
  - HDG for incompressible Navier–Stokes
  - Comparison of CPU times
  - Comparison of stability in presence of sharp fronts
- 2 Coupling of CG and HDG for heat equation
  - Coupled CG-HDG formulation for heat equation
  - Application of coupled formulation for conjugate heat transfer problem
- 3 Application to GFRP tubular cross-section
  - Problem statement
  - Radiosity
  - Numerical results
- 4 Summary

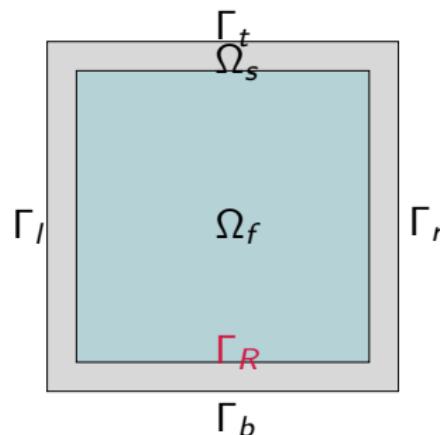
# Transmission and boundary conditions

- *Radiosity* equation governs the internal radiation. It is **non-linear algebraic** equation that depends on geometry.
- The transmission conditions for this problem are:

$$\theta_f - \theta_s = 0 \quad \text{on} \quad \Gamma_R,$$

$$-(\kappa_f \operatorname{grad} \theta_f) \cdot \mathbf{n}_f - (\kappa_s(\theta_s) \operatorname{grad} \theta_s) \cdot \mathbf{n}_s \\ - \frac{\epsilon}{1-\epsilon} (\sigma \theta_s^4 - R) = 0 \quad \text{on} \quad \Gamma_R.$$

$$R - \sigma \epsilon \theta^4 - (1-\epsilon) \int_{\Gamma_R} R \frac{\cos \gamma_x \cos \gamma_\xi}{2r} d\Gamma_R = 0.$$



# Transmission and boundary conditions

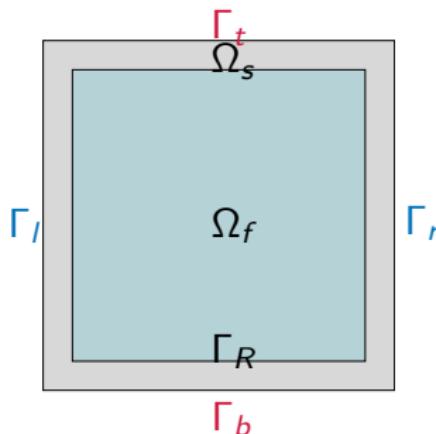
- *Radiosity* equation governs the internal radiation. It is **non-linear algebraic** equation that depends on geometry.
- The boundary conditions for this problem are:

$$\mathbf{u} = \mathbf{0} \quad \text{on} \quad \Gamma_R,$$

$$-(\kappa_s(\theta_s) \operatorname{grad} \theta_s) \cdot \mathbf{n} + h_a(\theta_s)(\theta_a - \theta_s)$$

$$+ \epsilon \sigma (\theta_a^4 - \theta_s^4) = 0 \quad \text{on} \quad \Gamma_t \cup \Gamma_b,$$

$$-(\kappa_s(\theta_s) \operatorname{grad} \theta_s) \cdot \mathbf{n} = 0 \quad \text{on} \quad \Gamma_l \cup \Gamma_r.$$



# Transmission and boundary conditions

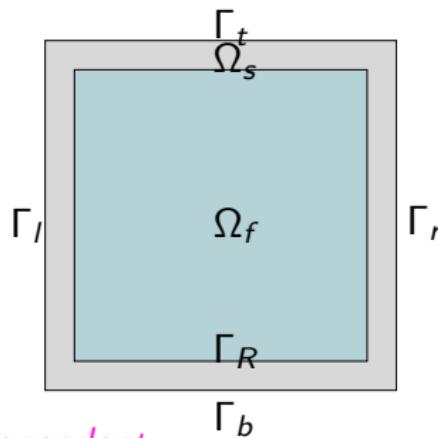
- *Radiosity* equation governs the internal radiation. It is **non-linear algebraic** equation that depends on geometry.
- The boundary conditions for this problem are:

$$\mathbf{u} = \mathbf{0} \quad \text{on} \quad \Gamma_R,$$

$$-(\kappa_s(\theta_s) \operatorname{grad} \theta_s) \cdot \mathbf{n} + h_a(\theta_s)(\theta_a - \theta_s)$$

$$+ \epsilon \sigma (\theta_a^4 - \theta_s^4) = 0 \quad \text{on} \quad \Gamma_t \cup \Gamma_b,$$

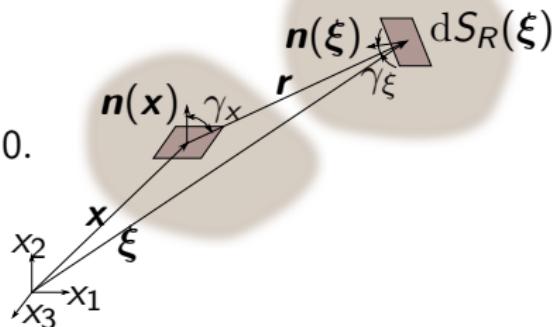
$$-(\kappa_s(\theta_s) \operatorname{grad} \theta_s) \cdot \mathbf{n} = 0 \quad \text{on} \quad \Gamma_l \cup \Gamma_r.$$



The material properties of GFRP are *temperature dependent*.

Radiosity equation can be expressed as follows:

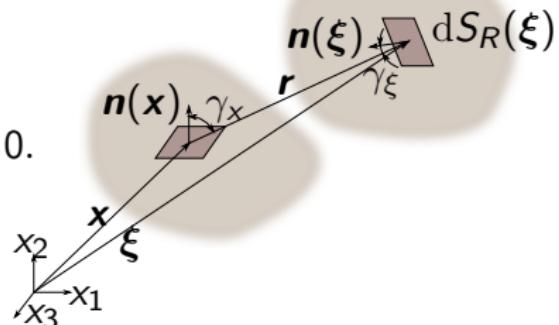
$$R - \sigma \epsilon \theta^4 - (1 - \epsilon) \int_{S_R} R \frac{\cos \gamma_x \cos \gamma_\xi}{\pi r^2} dS_R = 0.$$



Radiosity equation can be expressed as follows:

$$R - \sigma \epsilon \theta^4 - (1 - \epsilon) \int_{S_R} R \frac{\cos \gamma_x \cos \gamma_\xi}{\pi r^2} dS_R = 0.$$

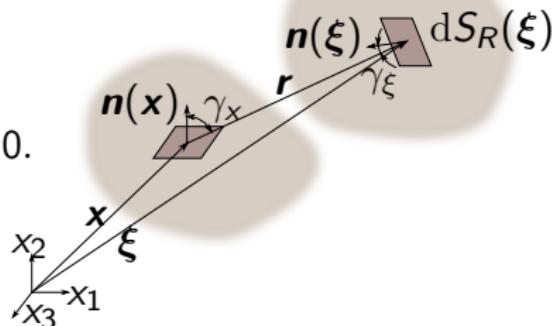
Two-dimensional particularisation yields:



$$R - \sigma \epsilon \theta^4 - (1 - \epsilon) \int_{\Gamma_R} R \frac{\cos \gamma_x \cos \gamma_\xi}{2r} d\Gamma_R = 0.$$

Radiosity equation can be expressed as follows:

$$R - \sigma \epsilon \theta^4 - (1 - \epsilon) \int_{S_R} R \frac{\cos \gamma_x \cos \gamma_\xi}{\pi r^2} dS_R = 0.$$



Two-dimensional particularisation yields:

$$R - \sigma \epsilon \theta^4 - (1 - \epsilon) \int_{\Gamma_R} R \frac{\cos \gamma_x \cos \gamma_\xi}{2r} d\Gamma_R = 0.$$

Imposed in weak sense:

$$\begin{aligned} & \left\langle \delta R^e, \frac{R^e}{(1 - \epsilon)} \right\rangle_{\Gamma_R^e} - \left\langle \delta R^e, \sigma \frac{\epsilon}{(1 - \epsilon)} (\theta^e)^4 \right\rangle_{\Gamma_R^e} \\ & - \sum_{\substack{k=1 \\ k \neq e}}^{n_I} \left\langle \delta R^e, \left\langle R^k, \frac{\cos \gamma^e \cos \gamma^k}{2r} \right\rangle_{\Gamma_R^k} \right\rangle_{\Gamma_R^e} = 0. \end{aligned}$$

Evolution of velocity and temperature with time

# Quantities of interest

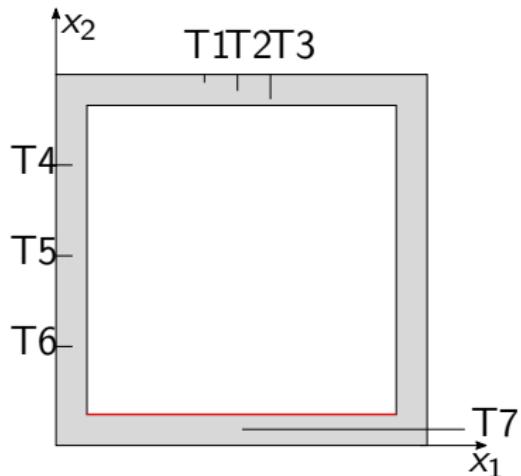


**Figure:** Locations of thermocouples in GFRP cross-section.

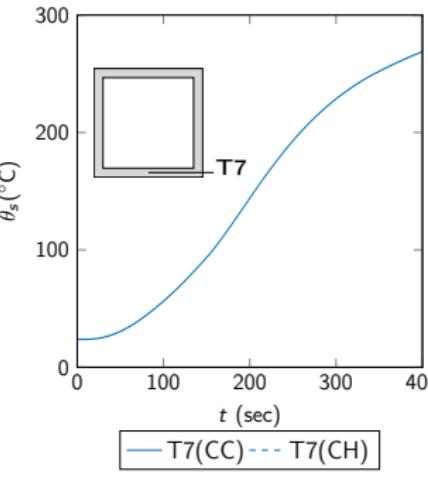
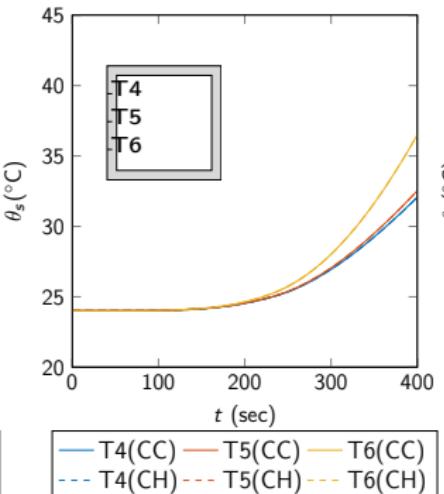
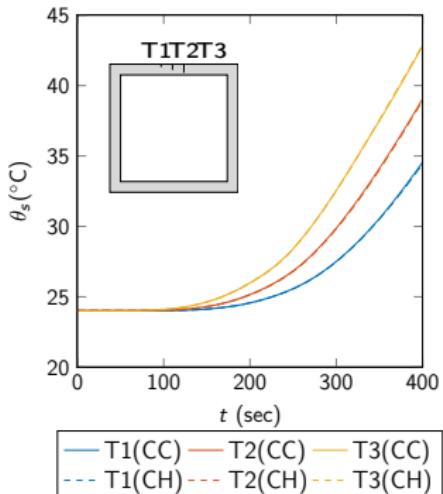
Thermocouple	$x_1$ (m)	$x_2$ (m)
T1	0.040	0.098
T2	0.050	0.096
T3	0.060	0.094
T4	0.004	0.075
T5	0.004	0.050
T6	0.004	0.025
T7	0.050	0.004

**Table:** Positions of different thermocouples.

$$\overline{Nu} = -\frac{1}{\theta_a - \theta_0} \int_{0.008}^{0.092} \frac{\partial \theta_s}{\partial x_2} ds,$$

$$\theta_a = \theta_0 + 345 \log(8 t + 1),$$

where  $t$  is in minutes.

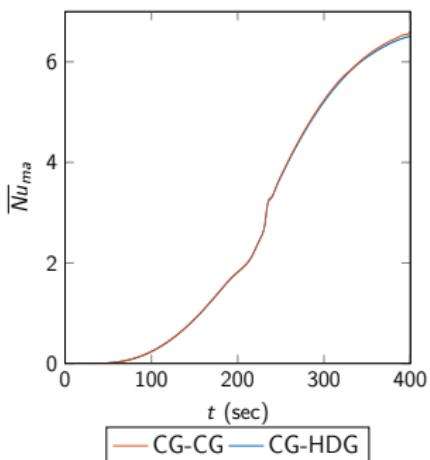


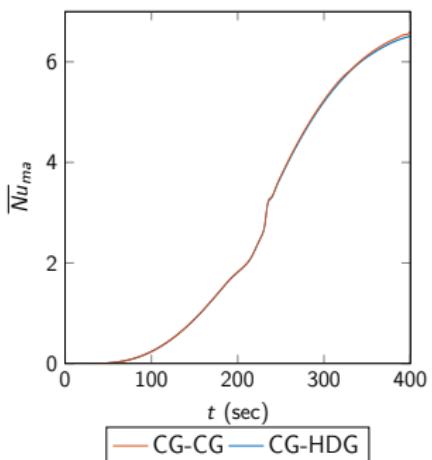
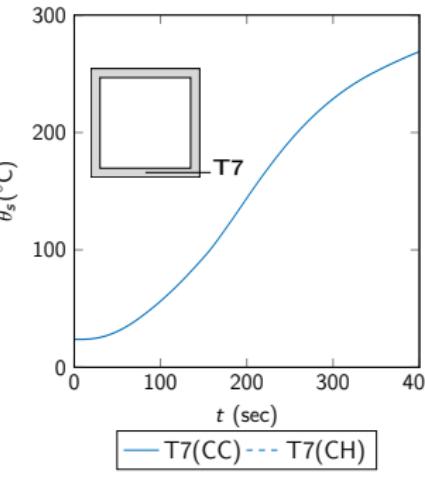
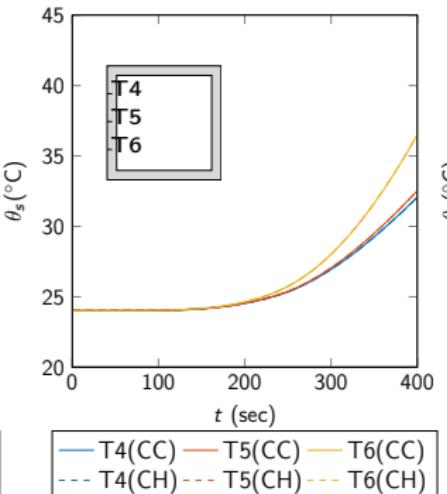
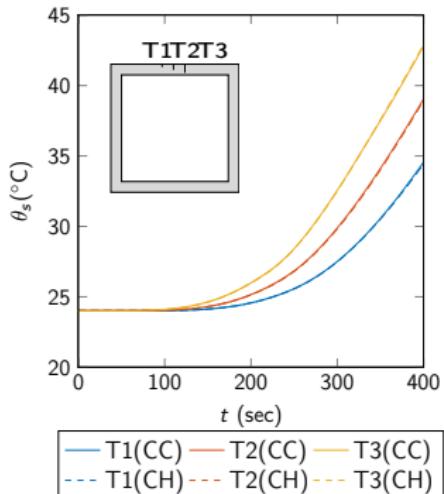
Comparison between  $\text{CG}(Q_2)\text{-HDG}(Q_1)$  and  $\text{CG}(Q_2)\text{-CG}(Q_2 Q_1)$

CC - CG-CG model

CH - CG-HDG model

$n_{el} = 20\,736$  and  $\Delta t = 0.0625/2^3$ .





Comparison between  $CG(Q_2)$ -HDG( $Q_1$ ) and  $CG(Q_2)$ - $CG(Q_2 Q_1)$

Quant	CH	CC
ndof	1 280 64	1 090 28
nnz	45 93 485	46 03 053
CPU Time	567 hr	854 hr
Solves	1 74 687	1 74 716
CPU Time/Solve	11.69 sec	17.61 sec

# Methodology for assessment of discretization error

- Method introduced in [Eça and Hoekstra \(2014\)](#) is used in the present work.
- Discretization error for a numerical method with convergence of order  $k$  in space and  $\mu$  in time is assumed to be,

$$\varepsilon_i(\phi) = \phi_i - \phi_a \approx c_{h,1} h_i + \dots + c_{h,k} h_i^k + c_{t,1} \Delta t_i + \dots + c_{t,\mu} \Delta t_i^\mu.$$

# Methodology for assessment of discretization error

- Method introduced in [Eça and Hoekstra \(2014\)](#) is used in the present work.
- Discretization error for a numerical method with convergence of order  $k$  in space and  $\mu$  in time is assumed to be,

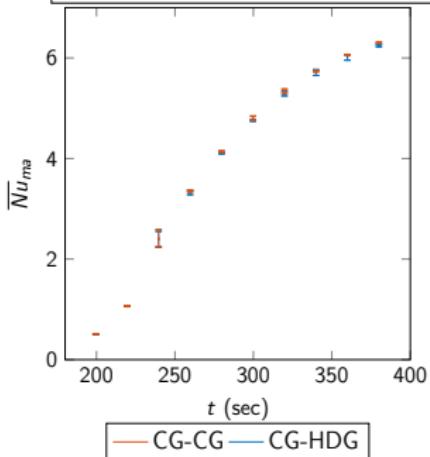
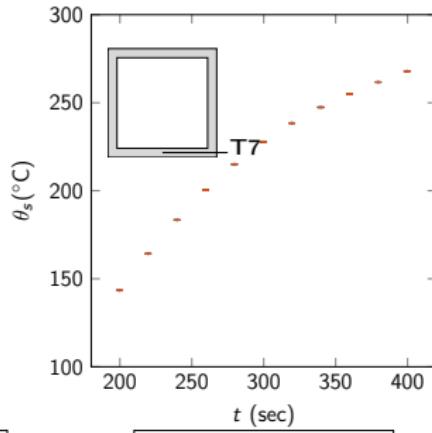
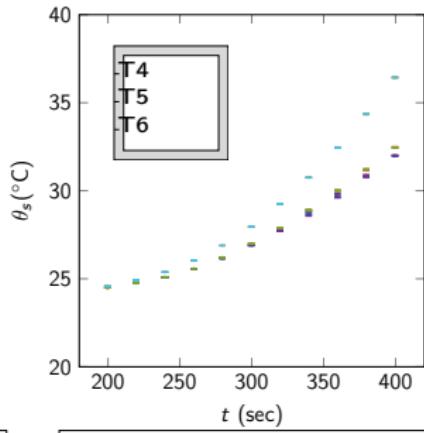
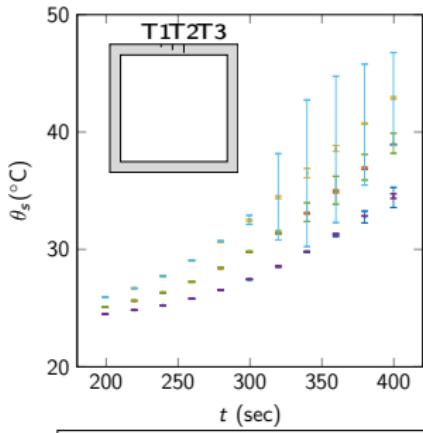
$$\varepsilon_i(\phi) = \phi_i - \phi_a \approx c_{h,1} h_i + \dots + c_{h,k} h_i^k + c_{t,1} \Delta t_i + \dots + c_{t,\mu} \Delta t_i^\mu.$$

- Standard deviation of the data points:

$$\hat{\sigma}_\varepsilon = \sqrt{\frac{\sum_{i=1}^{n_d} n_d w_i (\phi_i - (\phi_a + \dots + c_{h,k} h_i^k + \dots + c_{t,\mu} \Delta t_i^\mu))^2}{n_d - (k + \mu + 1)}}.$$

- Confidence intervals ( $\phi_i - U_\phi \leq \phi_a \leq \phi_i + U_\phi$ ) are established as:

$$U_\phi(\phi_i) = \begin{cases} 1.25 \varepsilon_i(\phi) + \hat{\sigma}_\varepsilon + |r|_i & \text{if } \hat{\sigma}_\varepsilon \leq \Delta_\phi, \\ 3 \frac{\hat{\sigma}_\phi}{\Delta_\phi} (\varepsilon_i(\phi) + \hat{\sigma}_\varepsilon + |r|_i) & \text{if } \hat{\sigma}_\varepsilon > \Delta_\phi. \end{cases}$$

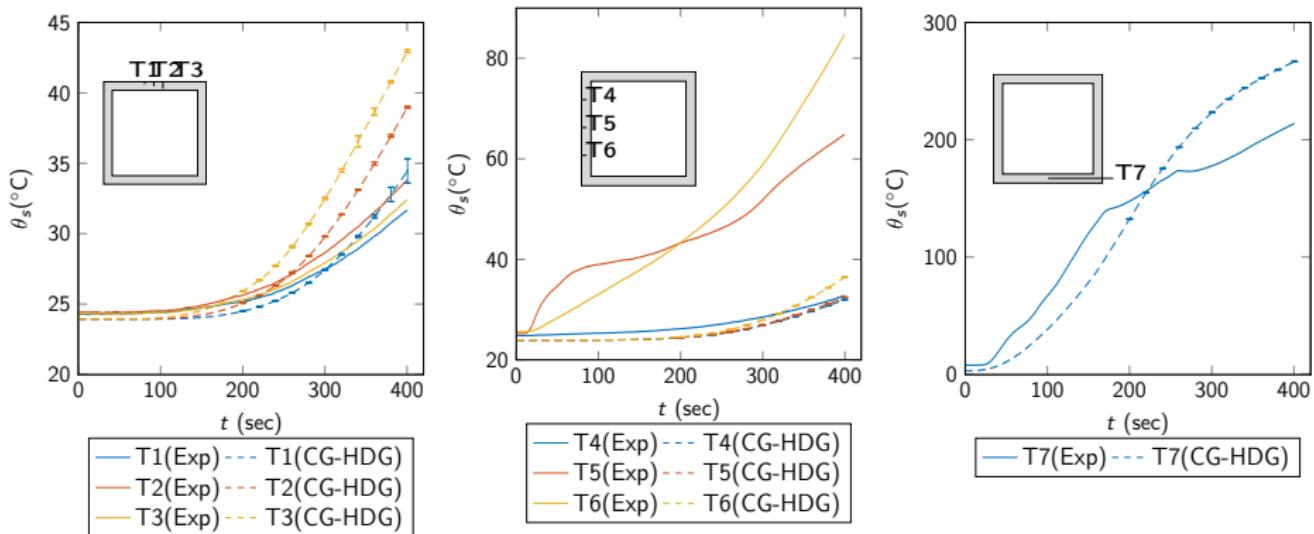


Comparison of discretization errors between  
 $CG(Q_2)$ - $HDG(Q_1)$  and  $CG(Q_2)$ - $CG(Q_2Q_1)$

CC - CG-CG model

CH - CG-HDG model

$n_{el} = 20\,736$  and  $\Delta t = 0.0625/2^3$ .



- Experimental validation of thermocouples with CG( $Q_2$ )-HDG( $Q_1$ ) model with **constant time step**.
- Discrepancies might be due to inaccuracies in **input conditions** and **experimental conditions**.
- Temperature in T2 is higher than T3 in experimental results.

# Conclusions

- The GFRP tubular cross-section results of considered coupled models are compared via *a posteriori* error estimation.
- Results showed a very similar accuracy for both coupled CG-HDG and CG-CG models.
- However, coupled CG-HDG model proved to **computationally more efficient** than CG-CG model.
- Numerical results of coupled CG-HDG model shows discrepancies with experimental data.

# Plan

- 1 Comparison of HDG and CG for incompressible Navier–Stokes
  - HDG for incompressible Navier–Stokes
  - Comparison of CPU times
  - Comparison of stability in presence of sharp fronts
- 2 Coupling of CG and HDG for heat equation
  - Coupled CG-HDG formulation for heat equation
  - Application of coupled formulation for conjugate heat transfer problem
- 3 Application to GFRP tubular cross-section
  - Problem statement
  - Radiosity
  - Numerical results
- 4 Summary

## Story of 3 years....

- Thermal response of GFRP tubular cross-section is considered in this work.
- Previous work suggested that resolving the fluid part is challenging.
- Computational potential of HDG compared to CG is assessed as a first step.
- Coupled CG-HDG formulation is proposed in order to couple fluid and solid domains in the GFRP problem.
- Final goal is achieved by predicting the thermal response of GFRP with the proposed coupled CG-HDG model and validated with the experimental data.

# Publications I

Paipuri, M., C. Tiago and S. Fernández-Méndez (2018). Numerical simulation of GFRP tubular section with high-order continuous and hybridizable discontinuous Galerkin methods along with experimental validation. (In preparation).

Paipuri, M., S. Fernández-Méndez and C. Tiago (2017). Comparison of high-order continuous and hybridizable discontinuous Galerkin methods in incompressible fluid flow problems. *Mathematics and Computers in Simulation*. (Submitted).

Paipuri, M., C. Tiago and S. Fernández-Méndez (2017). Coupling of continuous and hybridizable discontinuous Galerkin methods: Application to conjugate heat transfer problem. *Journal of Scientific computing*. (Submitted).

And 3 presentations in conferences and 1 conference paper.

# Acknowledgements

This project is funded by SEED consortium. SEED programme is an initiative of 8 universities [Partners], managed by the [EACEA] and financed by the European Commission with grant Ref. 2013-0043.

Thank you for the attention!



UNIVERSITAT POLITÈCNICA  
DE CATALUNYA



Co-funded by the  
Erasmus+ Programme  
of the European Union



# Plan

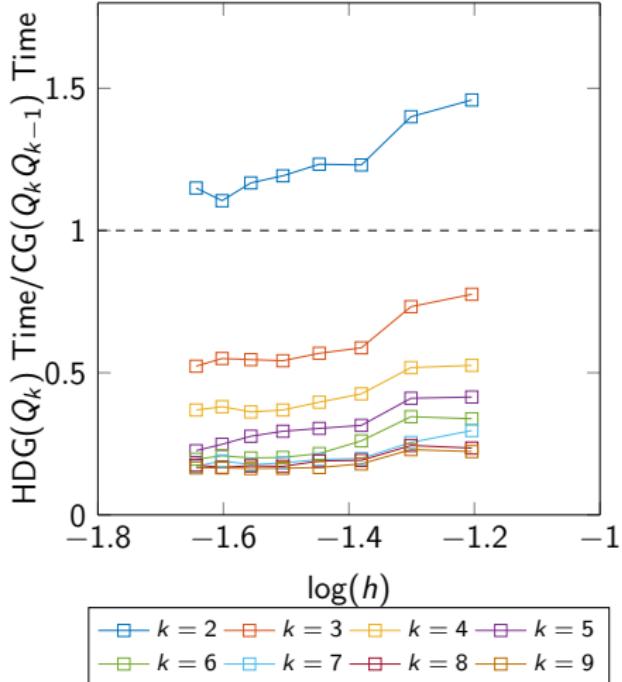
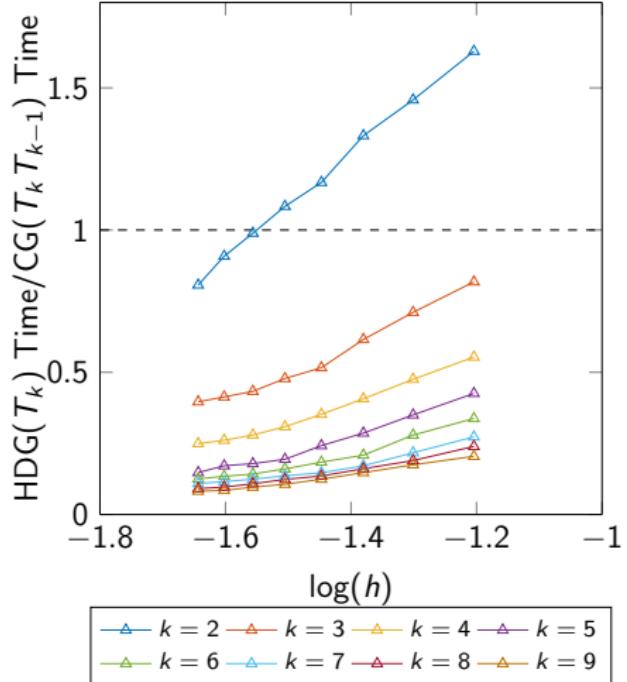
## 5 Additional results

- Computational efficiency
- Stability study
- Coupled CG-HDG formulation

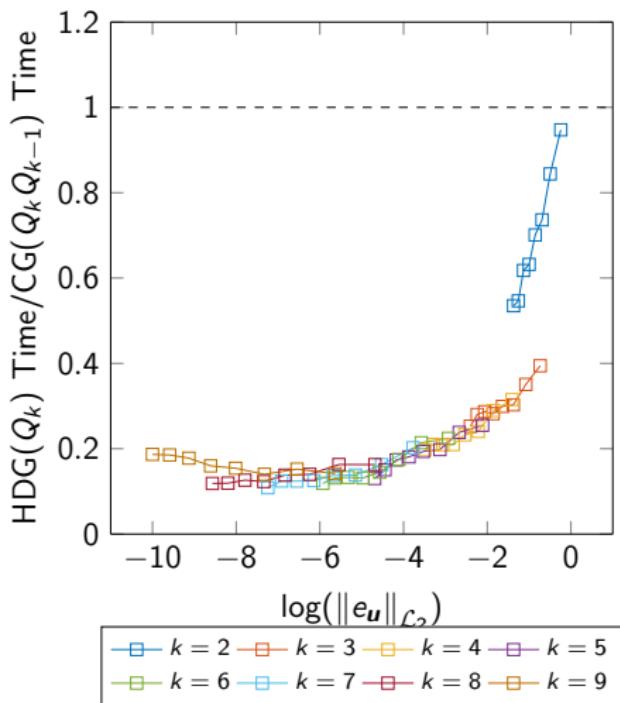
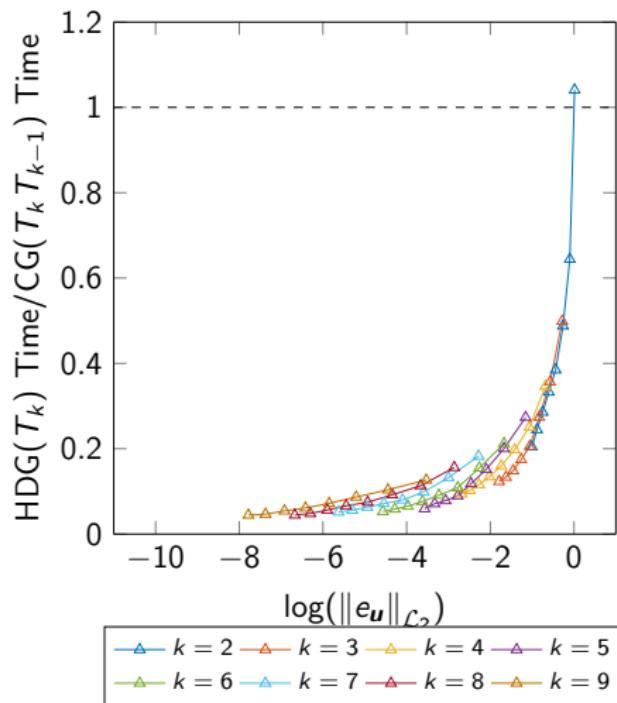
# Ratio of CPU times vs. element size for finer grids

$$\mathbf{u} = \begin{bmatrix} -\cos(70x_1)\sin(70x_2) \\ \sin(70x_1)\cos(70x_2) \end{bmatrix} \text{ in domain of } [0, 2]^2.$$

Mesh sizes considered are  $2/\{32, 40, 48, 56, 64, 72, 80, 88\}$ .



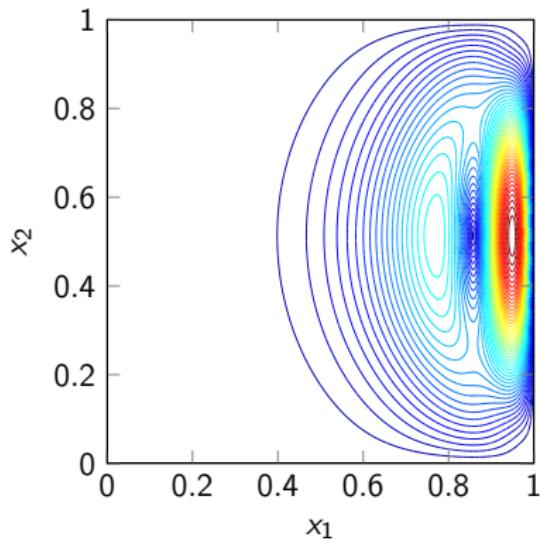
# Ratio of CPU times vs. element size for finer grids



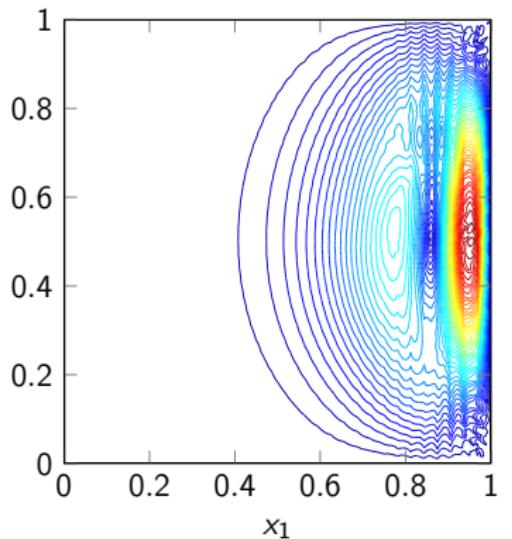
Isolines of velocity field at  $Re = 2500$  and  $k = 3$ ,  $h = 1/2^5$

No convergence obtained for steady state Navier–Stokes solver. **Unsteady Navier–Stokes** equation are solved until pseudo steady state is reached.

Navier–Stokes solution

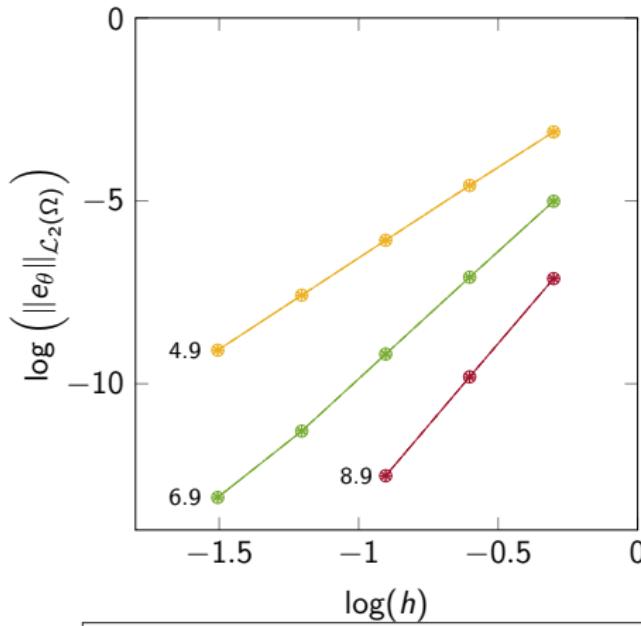


Navier–Stokes solution



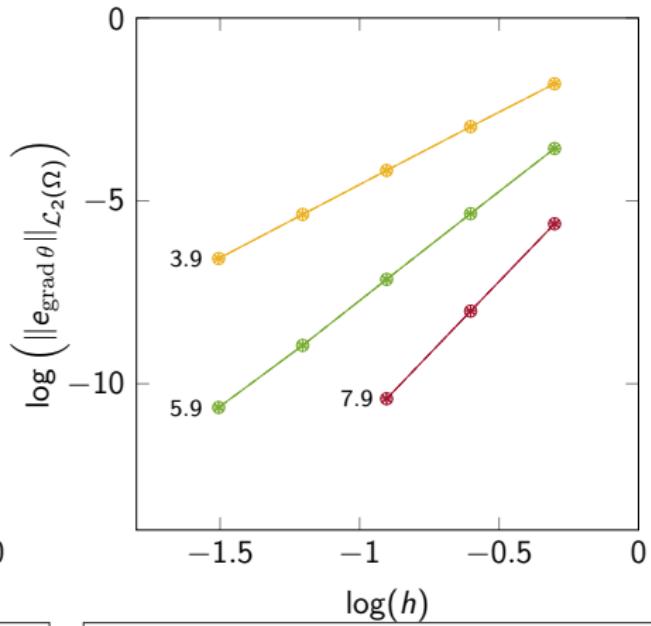
# Convergence for coupled $\text{CG}(T_{k+1})\text{-HDG}(T_k)$ model

## Single-face stabilisation approach



Legend:

- $\text{---} \circ \text{---}$   $k = 3, \tau = 1$
- $\text{---} + \text{---}$   $k = 3, \tau = 10$
- $\text{---} \times \text{---}$   $k = 3, \tau = 10^2$
- $\text{---} \ast \text{---}$   $k = 3, \tau = 10^3$
- $\text{---} \circ \text{---}$   $k = 5, \tau = 1$
- $\text{---} + \text{---}$   $k = 5, \tau = 10$
- $\text{---} \times \text{---}$   $k = 5, \tau = 10^2$
- $\text{---} \ast \text{---}$   $k = 5, \tau = 10^3$
- $\text{---} \circ \text{---}$   $k = 7, \tau = 1$
- $\text{---} + \text{---}$   $k = 7, \tau = 10$
- $\text{---} \times \text{---}$   $k = 7, \tau = 10^2$
- $\text{---} \ast \text{---}$   $k = 7, \tau = 10^3$



Legend:

- $\text{---} \circ \text{---}$   $k = 3, \tau = 1$
- $\text{---} + \text{---}$   $k = 3, \tau = 10$
- $\text{---} \times \text{---}$   $k = 3, \tau = 10^2$
- $\text{---} \ast \text{---}$   $k = 3, \tau = 10^3$
- $\text{---} \circ \text{---}$   $k = 5, \tau = 1$
- $\text{---} + \text{---}$   $k = 5, \tau = 10$
- $\text{---} \times \text{---}$   $k = 5, \tau = 10^2$
- $\text{---} \ast \text{---}$   $k = 5, \tau = 10^3$
- $\text{---} \circ \text{---}$   $k = 7, \tau = 1$
- $\text{---} + \text{---}$   $k = 7, \tau = 10$
- $\text{---} \times \text{---}$   $k = 7, \tau = 10^2$
- $\text{---} \ast \text{---}$   $k = 7, \tau = 10^3$

# Convergence for coupled CG( $T_{k+1}$ )-HDG( $T_k$ ) model

## All-face stabilisation approach

